Chemical Geology 513 (2019) 101–107

Contents lists available at ScienceDirect

Chemical Geology

journal homepage: www.elsevier.com/locate/chemgeo

Potassium isotopic compositions of international geological reference materials

Ying-Kui Xu[a,b,c], Yan Hu[b,*], Xin-Yang Chen[b], Tian-Yi Huang[b], Ronald S. Sletten[d], Dan Zhu[e,c], Fang-Zhen Teng[b,*]

[a] Center for Lunar and Planetary Sciences, Institute of Geochemistry, Chinese Academy of Sciences, Guiyang 550081, China
[b] Isotope Laboratory, Department of Earth and Space Sciences, University of Washington, Seattle, WA 98195, USA
[c] CAS Center for Excellence in Comparative Planetology, China
[d] Quaternary Research Center, Department of Earth and Space Sciences, University of Washington, Seattle, WA 98195, USA
[e] State Key Laboratory of Ore Deposit Geochemistry, Institute of Geochemistry, Chinese Academy of Sciences, Guiyang 550081, China

ARTICLE INFO

Editor: Catherine Chauvel

Keywords:
Potassium isotopes
MC-ICPMS
Reference materials
Seawater

ABSTRACT

There is a renewed interest in K isotope geochemistry driven by the advances in analytical precision and it is emerging as a useful tracer in a variety of disciplines ranging from Earth sciences to biology. However, high-quality K isotopic data for reference materials are still limited but highly needed. Here, we report high-precision stable K isotopic compositions ($\delta^{41}K$) for 23 commercially available international reference materials, including igneous, sedimentary, and metamorphic rocks, as well as an in-house seawater standard. Potassium in digested samples was separated by cation-exchange chromatography with Bio-Rad AG50W-X8 (200–400 mesh) resin in 0.5 N HNO_3 media. Potassium isotopes were measured on a Nu Plasma II high-resolution MC-ICPMS. The reproducibility of K isotopic analysis, based on over one year of measurements of pure K solutions and rock standards, was ≤0.06‰ (95% confidence interval). Synthetic solutions made by mixing single element standards to represent various rock matrices confirmed the accuracy of our methods. The 23 reference materials have $\delta^{41}K$ values ranging from −0.562‰ to −0.253‰ and the seawater standard has a much higher $\delta^{41}K$ value of 0.143‰. The comprehensive dataset presented here provides a reference for quality control and inter-laboratory comparison of high-precision K isotopic analyses for future studies.

1. Introduction

Potassium (K) is the fifteenth most abundant element in the bulk Earth, the eighth in the crust, and the sixth in the ocean (Culkin and Cox, 1966; McDonough and Sun, 1995; Rudnick and Gao, 2003). It is also an essential nutrient for metabolic and physiological reactions in organisms (Edelmann, 1971). Potassium has two stable isotopes ^{39}K (93.25%) and ^{41}K (6.73%), as well as one radioactive isotope ^{40}K (0.02%) (Berglund and Wieser, 2011). Early studies of K isotopes focused mainly on evaporation and condensation processes during planetary formation (e.g., Humayun and Clayton, 1995b) using Thermal Ionization Mass Spectrometry (TIMS) (Garner et al., 1975) or Secondary Ion Mass Spectrometry (SIMS) (Humayun and Clayton, 1995a). Analytical uncertainties of these measurements are larger than 0.5‰ (2SD), which cannot distinguish most K isotopic variation in terrestrial samples (Humayun and Clayton, 1995a,b).

Recently, high-precision Multi-Collector Inductively Coupled Plasma Mass Spectrometry (MC-ICPMS) was applied to measure K isotopes. The strong argide interferences (e.g. ArH^+) on K^+ peaks were suppressed by either the collision cell (Richter et al., 2014; Li et al., 2016; Wang and Jacobsen, 2016a) or by the "cold plasma" method (Hu et al., 2018; Morgan et al., 2018; Chen et al., 2019), and precision has been improved by one order of magnitude, making it possible to resolve natural K isotopic variations. To date, 3‰ variation in $^{41}K/^{39}K$ ratios has been reported for samples of extraterrestrial materials (meteorites, lunar rocks, and tektites) and terrestrial rocks, sediments, seawater, as well as biological materials (Teng et al., 2017). These results have been used to constrain a variety of geological and biological processes such as the Moon-forming event and submarine weathering of oceanic crust and marine sediments (Wang and Jacobsen, 2016b; Li, 2017; Li et al., 2017; Parendo et al., 2017; Morgan et al., 2018; Santiago Ramos et al., 2018).

Non-traditional stable isotope systems often have relatively small variations in nature, particularly during high-temperature processes

* Corresponding authors.
E-mail addresses: yanhu@u.washington.edu (Y. Hu), fteng@u.washington.edu (F.-Z. Teng).

https://doi.org/10.1016/j.chemgeo.2019.03.010
Received 20 October 2018; Received in revised form 13 February 2019; Accepted 7 March 2019
Available online 08 March 2019
0009-2541/

(Teng et al., 2017), and their application has been limited by analytical accuracy. This limitation is especially the case for K isotopes. Since K only has two stable isotopes, the double-spike technique cannot be used to evaluate mass-dependent fractionation behavior or correct for instrumental fractionation. One way to ensure analytical accuracy is to measure well-characterized, lithologically-diverse reference materials. For K isotopes, there are currently only six bulk rock standards from United States Geological Survey (USGS) that have been analyzed independently by three laboratories (Li et al., 2016; Wang and Jacobsen, 2016a,b; Hu et al., 2018; Morgan et al., 2018; Santiago Ramos et al., 2018; Chen et al., 2019). Furthermore, there may be greater uncertainty when converting their $\delta^{41}K$ values to the same reference scale because these standards have been measured against several different bracketing standards.

Considering the limited database and relatively large uncertainty of published data, this study presents systematic high-precision and high-accuracy measurements on K isotopic compositions in a suite of 23 geological standards covering wide lithological variation, as well as an in-house Hawaiian seawater standard. The rock standards include 19 igneous rocks, three sedimentary rocks, and one metamorphic rock; they are from the USGS, Geological Society of Japan (GSJ), Centre de Recherches Pétrographiques et Géochimiques (CRPG) of France, Association Nationale de la Recherche Technique (ANRT) of France, Canadian Certified Reference Materials Project (CCRMP), and National Research Center for Geoanalysis (NRCGA) of China. These are commonly used reference materials that are commercially available. They were measured and reported against the Standard Reference Material (SRM) 3141a from National Institute of Standards and Technology (NIST), following the recommendation of Li et al. (2016) and Hu et al. (2018). This dataset thus serves as a comprehensive reference for data quality control and inter-laboratory comparison of high-precision K isotopic analysis.

2. Analytical methods

Sample preparation was performed in a class-100 laminar flow fume hood in a class-10,000 clean laboratory in the Isotope Laboratory at the University of Washington, Seattle. Savillex screw-top Teflon beakers, double-distilled acids, and Milli-Q water (18.2 MΩ) were used to maintain low blank levels.

2.1. Sample dissolution

Typically, 5–30 mg of sample powders were weighed and digested in Teflon beakers using a mixture of concentrated HF-HNO_3 (optima-grade, 3:1 v/v). For samples containing organic matter, several drops of optima-grade H_2O_2 were added. These beakers were capped and heated on a hotplate at 120 °C for approximately three days, periodically vibrated in an ultrasonic bath, and dried at 100 °C. Samples were then treated with aqua regia (optima-grade HCl-HNO_3, 3:1 v/v) until complete dissolution. After that, they were refluxed in concentrated HNO_3 and dried again. Finally, samples were dissolved in 0.5 N HNO_3, in preparation for the cation-exchange columns.

2.2. Column chemistry

Purification of K was achieved by cation-exchange chromatography with a similar method adapted from Strelow et al. (1970). A pre-cleaned Bio-Rad Poly-Prep polyethylene column was packed with 2 ml (0.8 × 4 cm) pre-cleaned Bio-Rad AG50W-X8 (200–400 mesh) resin. The resin was conditioned by 10 ml 0.5 N HNO_3. Sample solutions were then loaded on the resin and eluted by 0.5 N HNO_3. Matrix elements were eluted in the first 13 ml 0.5 N HNO_3; the subsequent 22 ml fractions containing the K was collected; and, finally, the remaining elements were washed off the resin by 10 ml of 6 N HCl. The detailed procedure of column chemistry is provided in Table 1.

Table 1
Potassium cation-exchange column procedure.

Action	Purpose
10 ml MQ H_2O	Clean column
10 ml 6 N HNO_3	Clean column
10 ml MQ H_2O	Clean column
Fill 2 ml resin in MQ H_2O	Load resin
10 ml MQ H_2O	Clean resin
10 ml 6 N HNO_3	Clean resin
10 ml MQ H_2O	Clean resin
10 ml 0.5 N HNO_3	Condition
Load sample (1 ml 0.5 N HNO_3)	Load sample
13 ml 0.5 N HNO_3	Elute matrices
22 ml 0.5 N HNO_3	Collect K
10 ml 6 N HCl	Wash resin
10 ml MQ H_2O	Wash resin

Table 2
Potassium isotopic tests of pure K and synthetic samples.

Sample		$\delta^{41}K_{FZT\ K\text{-}1}$ (‰)	2SD (‰)	95% c.i. (‰)	n
FZT K-1	I #1	−0.008	0.116	0.055	6
	I #1 (Replicate)	−0.024	0.148	0.060	5
	I #1 (Replicate)	0.013	0.106	0.051	7
	I #2	0.015	0.052	0.050	6
	I #2 (Replicate)	0.005	0.082	0.054	5
	I #2 (Replicate)	0.001	0.115	0.050	6
FZT K-1 with multiple elements	II #1	−0.011	0.103	0.042	7
	II #2	−0.019	0.088	0.042	7
	II #3	0.015	0.091	0.045	6
	II #4	0.001	0.060	0.042	7
FZT K-1 with natural rock matrices	III #1	0.013	0.032	0.045	6
	III #2	0.031	0.074	0.042	7
	III #3	0.040	0.098	0.045	6
	III #3 (Duplicate)	−0.033	0.035	0.061	4
	III #4	0.025	0.105	0.049	5

Notes:
I #1 and I #2: FZT K-1 after two and three times of column chemistry, respectively.
II #1–II #4: FZT K-1 mixed with multiple elements.
III #1–III #4: FZT K-1 mixed with natural rock matrices (#1: BHVO-1 matrices; #2: AGV-1 matrices; #3: GSP-1 matrices; #4: G-2 matrices).
Replicate: repeat sample dissolution, column chemistry, and instrumental analyses.
Duplicate: repeat analysis on the same purified sample solution during different analytical sessions.
95% c.i.: two standard error corrected by the Student's t factor (Platzner, 1997) and representing 95% confidence interval.
2SD: two standard deviation.
n: number of analyses.

The column separation procedure was calibrated using an in-house KNO_3 standard solution (FZT K-1) from Spex CertiPrep® and three geostandards from NRCGA (gabbro GBW07112, granodiorite GBW07111, and granite GBW07103). Eluent fractions were measured using a Perkin-Elmer 3300 Dual View Inductively Coupled Plasma Optical Emission Spectrometry (DV ICP-OES) calibrated with Spex CertiPrep® standards. The elution curves indicate that K is effectively separated from other major elements (Fig. 1). Titanium and Na were eluted before K, and other major elements (Fe, Mg, Ca, Mn and Al) were retained in the resin. However, among all elements measured, Rb cannot be quantitatively separated from K because both have similar resin-eluent partition coefficients. Nevertheless, Rb/K ratio of most natural samples is < 1%, and the doping tests by Hu et al. (2018)

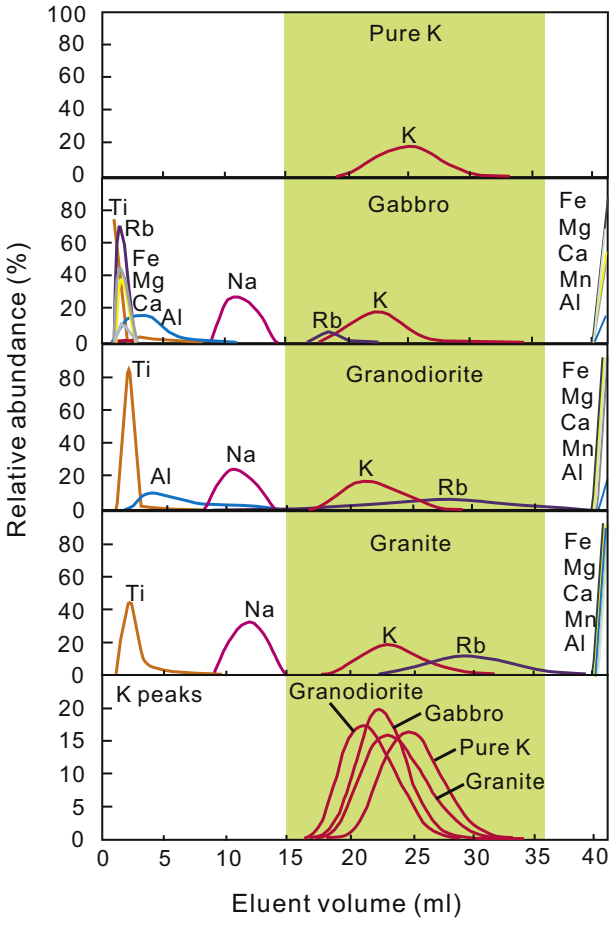

Fig. 1. Elution curves for Spex K standard, gabbro, granodiorite, and granite. Over 99.73% K was collected from 15 to 36 ml interval. All matrix elements are completely removed with the exception of Rb.

confirmed that a Rb/K ratio of up to one does not affect the measured $\delta^{41}K$ values within analytical uncertainties. The column separation was repeated twice to achieve an effectively pure K solution. The average K yield of our analytical protocol is 99.7 ± 1.1% (2SD, $n = 4$). The procedural blank, including sample dissolution, column chemistry, and instrumental analysis varies from 0.63 to 9.4 ng; this is insignificant compared to the amount of K (100–200 μg) loaded onto the columns.

Large isotope fractionation has been observed during ion-exchange chromatography in many isotope systems, e.g., Li, Mg, Ca, and Rb (Taylor and Urey, 1938; Teng et al., 2007; Morgan et al., 2011; Zhang et al., 2018). The K isotopic variation during column chemistry was examined here to ensure there is no artificial isotope fractionation induced due to incomplete recovery. Two individual 1000 μg FZT K-1 solutions were processed through the column and the 22 ml K fraction was collected in five intervals with volumes of 7 ml, 3 ml, 2 ml, 2 ml, and 8 ml; and volumes of 8 ml, 3 ml, 2 ml, 2 ml, and 7 ml. Analyses of these K cuts suggest that the light K isotope was preferentially eluted off the resin, followed by the remaining heavy K isotope (Fig. 2). This is opposite to the behaviors of the K isotopes on a Dionex CS-16 cation exchange column (Morgan et al., 2018) as well as to other non-traditional stable isotopes such as Li, Mg and Ca for which the heavier isotopes are preferentially released from the resin (Taylor and Urey, 1938; Russell and Papanastassiou, 1978; Teng et al., 2007; Morgan et al., 2011). However, our result is consistent with Rb isotope fractionation on a Sr-spec resin in HNO_3 media (Zhang et al., 2018). These different fractionation behaviors might reflect the influence of the large ionic radii of K^+ and Rb^+ on the equilibrium isotope partitioning between the resin and eluent, which leads to the preference of heavier isotope

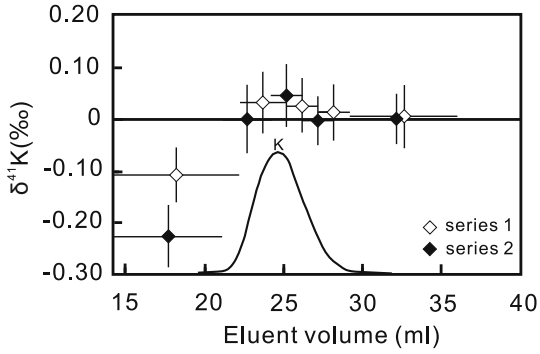

Fig. 2. K isotope fractionation during column chemistry. Horizontal bars represent the collecting volume range; vertical bars represent 95% c.i. of K isotopic value.

for the resin. Regardless of the mechanisms responsible for the differing fractionation behaviors, full recovery of K during column chemistry is required. The 22-ml fraction in our column procedure collected the entire K fraction eluted, thereby avoiding any potential column fractionation artifacts.

2.3. Mass spectrometry

The K isotopes were measured on a Nu Plasma II HR-MC-ICPMS at the Isotope Laboratory, University of Washington, Seattle. Analytical details for this instrument are presented in Hu et al. (2018) and a brief description is given below.

The K isotopic compositions of the purified sample solutions were measured using "cold plasma" at a lowered RF power to suppress interferences from isobaric argides ($^{38}Ar^1H^+$ on $^{39}K^+$ and $^{40}Ar^1H^+$ on $^{41}K^+$, respectively). High resolution mode was used to minimize residual argide interferences thereby providing an interference-free, peak shoulder for the K isotope analysis (Hu et al., 2018). "Dry plasma" sample introduction was used to increase sensitivity and further reduce argide formation, which consists of a DSN-100 desolvation nebulizer system fitted with a PFA spray chamber and a MicroMist glass nebulizer. Sample solutions and bracketing standards were diluted using a same batch of 3% HNO_3 to a K concentration of 5 to 8 ppm, which produces 5 to 11 V of ^{39}K signal. On-peak zero on mass 41 varies mostly between -8×10^{-4} and -1.5×10^{-3} V and that on mass 39 is typically around -3×10^{-3} V; these are negligible compared to the signals of sample solutions.

Instrumental mass fractionation was corrected by sample-standard bracketing technique. The sample-standard sequence for each sample was repeated n times ($n \geq 4$). The K isotopic composition is expressed in delta (δ) notation following previous recommendation (Teng et al., 2017):

$$\delta^{41}K(‰) = \left\{ \frac{(^{41}K/^{39}K)_{sample}}{(^{41}K/^{39}K)_{standard}} - 1 \right\} \times 1000 \quad (1)$$

The normalization standard used for natural reference materials is NIST SRM 3141a and that used for synthetic samples is Spex CertiPrep® KNO_3 solution (FZT K-1).

Analytical uncertainties are reported as both 2SD (standard deviation of n repeated sample analyses during an analytical session) and 95% confidence interval (c.i.). The 95% c.i. is calculated from the standard deviation of all bracketing standard measurements during an analytical session and is corrected by the Student's t factor (Platzner, 1997) (95%c. i. $= t\frac{SD}{\sqrt{n}}$) (see Hu et al., 2018 for more details). The reproducibility of K isotopic measurements of pure K solutions and rock standards over a year was ≤0.06‰ (95% c.i.) (Hu et al., 2018). All duplicates (repeat analysis on the same purified sample solution during different analytical sessions) and replicates (repeat sample dissolution,

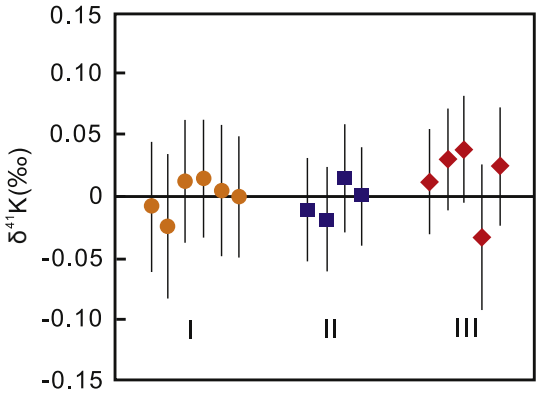

Fig. 3. K isotopic compositions of synthetic solutions with the expected true value of zero. I: FZT K-1 solution after passing the column successively two or three times; II: FZT K-1 mixed with multiple elements; III: FZT K-1 mixed with natural rock matrices (BHVO-1, AGV-1, GSP-1 and G-2 matrices). Data are reported in Table 2.

column chemistry, and instrumental analysis) are reproducible within 0.06‰.

3. Evaluation of analytical accuracy

To verify that the K isotopic data are both precise and accurate, we carried out the following three sets of tests:

First, we processed a pure K solution through the entire analytical procedure to assess whether any isotope fractionation occurred during column chemistry. For this purpose, a sample containing 200 μg K is prepared from Spex CertiPrep® KNO_3 solution (FZT K-1) and then successively passed through the column chemistry either two or three times. The $\delta^{41}K$ values of the collected K fractions are −0.006 ± 0.037‰ (2SD, $n = 3$) and 0.007 ± 0.014‰ (2SD, n = 3), respectively, indicating that our column procedure does not induce analytical artifact for pure K solution (I in Fig. 3).

In the second test, we used synthetic solutions that mimic various rock compositions in nature to evaluate whether our column chemistry effectively removes matrix elements. Two types of synthetic solutions were prepared: four individual batches of pure K solution (FZT K-1) were mixed with multiple elements (100 μg K, 100 μg Na, 100 μg Mg, 100 μg Fe, 100 μg Ca, 100 μg Al, 10 μg Mn, 10 μg Ti) (II in Fig. 3); the pure K solution FZT K-1 was added to the eluted matrix fractions of four USGS standards in quantities that matched the K masses in the original samples (128 μg K in a matrix of 28.79 mg BHVO-1 basalt, 120 μg K in a matrix of 4.91 mg AGV-1 andesite, 228 μg K in a matrix of 5.00 mg GSP-1 Granodiorite, and 119 μg K in a matrix of 3.20 mg G-2 granite) (III in Fig. 3). Both sets of solutions were processed through column chemistry and analyzed against FZT K-1. These tests yielded $\delta^{41}K$ values that range from −0.033‰ to 0.040‰, with a mean of 0.007 ± 0.048‰ (2SD, $n = 9$), further validating the accuracy of our column chemistry.

For the final test, we processed and measured well-characterized reference materials for inter-laboratory comparison, including a seawater standard and 12 rock standards (BHVO-1, BCR-1, AGV-1, GSP-1, G-2, GS-N, RGM-1, QLO-1, MAG-1, SCo-1, SGR-1 and SDC-1). Our data are consistent with those reported by other laboratories within uncertainty (Li et al., 2016; Wang and Jacobsen, 2016b; Morgan et al., 2018; Santiago Ramos et al., 2018; Chen et al., 2019) (Fig. 4), confirming that our methods for chemical separation and instrumental analysis are consistent with other laboratories. Furthermore, our greater precision provides tighter constraints on the published values.

4. K isotopic compositions of reference materials

The K isotopic compositions of 23 reference materials and seawater

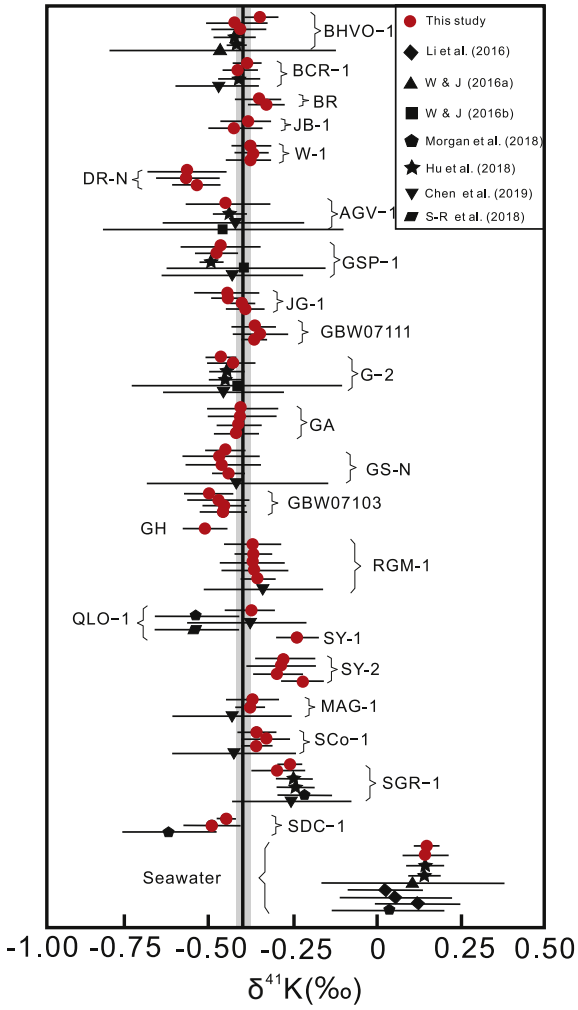

Fig. 4. K isotopic compositions of reference materials, together with data reported by other laboratories. Precision is plotted as 2SD for comparison. The solid line and shaded area highlight the $\delta^{41}K$ of the mantle as represented by standard BHVO-1 (−0.411 ± 0.012‰, 95% c.i.). Data are reported in Table 3.

are reported in Table 3 and plotted in Fig. 4, together with published data when available. Notably, 11 out of the 23 reference materials have not been analyzed for K isotopes previously.

To make an internally consistent database, we compile the reference materials' data reported in this study and in Hu et al. (2018), then calculate an average $\delta^{41}K$ value and associated uncertainty for each reference material. These are calculated as an error-weighted mean of replicate and duplicate analyses using the following equations:

$$\text{error} - \text{weighted mean} = \frac{\sum \frac{X}{SD^2}}{\sum \frac{1}{SD^2}} \quad (2)$$

$$2SD \text{ of error} - \text{weighted mean} = 2 \times \sqrt{\frac{1}{\sum \frac{1}{SD^2}}} \quad (3)$$

$$95\%\text{c. i. of error} - \text{weighted mean} = \sqrt{\frac{1}{\sum \frac{1}{(95\%\text{c.i.})^2}}} \quad (4)$$

where X is the $\delta^{41}K$ value of each analysis; SD is standard deviation; and 95% c.i. represents 95% confidence interval.

The igneous reference materials range in composition from mafic to felsic, and their $\delta^{41}K$ values vary from −0.562‰ to −0.253‰, with the diorite (DR-N) having the lowest $\delta^{41}K$ and two syenites (SY-1 and SY-2) having the highest $\delta^{41}K$ (Fig. 4). In comparison, basalts display a

Table 3
Potassium isotopic compositions of reference materials and seawater.

Sample	Description	$\delta^{41}K_{3141a}$ (‰)	2SD (‰)	95% c.i. (%)	n
BHVO-1	Basalt, USGS	−0.355	0.044	0.013	12
Replicate		−0.425	0.089	0.046	7
Replicate		−0.417	0.081	0.056	5
Literature-1		−0.430	0.060	0.050	5
Literature-1		−0.420	0.020	0.050	4
Average		−0.411	0.017	0.012	
Literature-2		−0.467	0.348		84
BCR-1	Basalt, USGS	−0.400	0.040	0.013	12
Replicate		−0.421	0.050	0.054	6
Literature-1		−0.420	0.060	0.030	8
Average		−0.411	0.028	0.012	
Literature-6		−0.490	0.120	0.050	8
BR	Basalt, CRPG	−0.370	0.068	0.051	6
Replicate		−0.335	0.052	0.047	4
Average		−0.348	0.041	0.034	
JB-1	Basalt, GSJ	−0.403	0.075	0.056	5
Replicate		−0.432	0.083	0.047	4
Average		−0.416	0.056	0.036	
W-1	Diabase, USGS	−0.394	0.046	0.056	5
Replicate		−0.388	0.045	0.047	4
Replicate		−0.390	0.068	0.032	7
Average		−0.391	0.029	0.024	
DR-N	Diorite, ANRT	−0.576	0.114	0.046	6
Replicate		−0.574	0.091	0.038	6
Replicate		−0.550	0.071	0.050	5
Average		−0.562	0.050	0.025	
AGV-1	Andesite, USGS	−0.450	0.120	0.046	7
Literature-1		−0.446	0.053	0.018	12
Average		−0.447	0.049	0.017	
Literature-3		−0.462	0.368		11
Literature-6		−0.430	0.224	0.080	10
GSP-1	Granodiorite,	−0.478	0.122	0.046	7
Replicate	USGS	−0.486	0.064	0.031	6
Literature-1		−0.498	0.039	0.020	10
Average		−0.494	0.032	0.016	
Literature-3		−0.410	0.242		13
Literature-6		−0.440	0.140	0.050	10
JG-1	Granodiorite, GSJ	−0.456	0.095	0.050	5
Replicate		−0.456	0.042	0.052	5
Replicate		−0.412	0.032	0.054	6
Duplicate		−0.404	0.054	0.032	7
Average		−0.425	0.022	0.022	
GBW07111	Granodiorite,	−0.383	0.063	0.048	6
Replicate	NRCGA	−0.360	0.077	0.053	5
Replicate		−0.380	0.029	0.029	6
Average		−0.379	0.025	0.023	
G-2	Granite, USGS	−0.472	0.039	0.020	10
Replicate		−0.447	0.066	0.053	5
Literature-1		−0.454	0.053	0.041	6
Literature-1		−0.458	0.052	0.027	6
Average		−0.462	0.025	0.014	
Literature-3		−0.423	0.315		12
Literature-6		−0.460	0.166	0.040	19
GA	Granite, CRPG	−0.411	0.110	0.050	5
Replicate		−0.416	0.111	0.039	6
Duplicate		−0.424	0.066	0.059	4
Replicate		−0.432	0.062	0.042	7
Average		−0.425	0.039	0.023	
GS-N	Granite, ANRT	−0.460	0.064	0.056	4
Replicate		−0.480	0.120	0.059	4
Duplicate		−0.473	0.112	0.042	5
Replicate		−0.461	0.040	0.030	6
Average		−0.463	0.031	0.021	
Literature-6		−0.430	0.265	0.080	13
GBW07103	Granite, NRCGA	−0.508	0.071	0.048	6
Duplicate		−0.479	0.088	0.051	5
Replicate		−0.462	0.068	0.053	5
Replicate		−0.465	0.073	0.038	5
Average		−0.478	0.037	0.023	
GH	Granite, CRPG	−0.522	0.062	0.035	7
RGM-1	Rhyolite, USGS	−0.384	0.096	0.046	6
Duplicate		−0.380	0.051	0.055	4
Duplicate		−0.384	0.102	0.051	5
Replicate		−0.374	0.097	0.048	6
Replicate		−0.368	0.055	0.047	4
Average		−0.376	0.031	0.022	
Literature-6		−0.350	0.150	0.040	16
QLO-1		−0.391	0.073	0.042	5
Literature-5		−0.550	0.140		4
Literature-6	Quartz latite, USGS	−0.400	0.119	0.040	11
Literature-7		−0.550	0.140		4
SY-1	Syenite, CCRMP	−0.253	0.059	0.035	6
SY-2	Syenite, CCRMP	−0.274	0.097	0.050	5
Replicate		−0.292	0.114	0.048	6
Duplicate		−0.296	0.088	0.047	4
Replicate		−0.252	0.059	0.038	6
Average		−0.270	0.041	0.023	
MAG-1	Marine mud,	−0.378	0.077	0.046	6
Replicate	USGS	−0.387	0.035	0.030	6
Average		−0.385	0.032	0.025	
Literature-6		−0.440	0.132	0.040	13
SCo-1	Shale, USGS	−0.364	0.056	0.056	4
Replicate		−0.339	0.074	0.048	6
Replicate		−0.366	0.048	0.035	7
Average		−0.360	0.033	0.025	
Literature-6		−0.430	0.150	0.040	16
SGR-1	Shale, USGS	−0.267	0.038	0.018	12
Replicate		−0.307	0.086	0.047	4
Literature-1		−0.253	0.054	0.046	5
Literature-1		−0.251	0.055	0.040	6
Average		−0.264	0.026	0.015	
Literature-5		−0.220	0.080		4
Literature-6		−0.260	0.168	0.060	10
SDC-1	Mica schist, USGS	−0.458	0.028	0.019	11
Replicate		−0.497	0.089	0.048	6
Average		−0.461	0.027	0.017	
Literature-5		−0.630	0.140		2
Hawaiian seawater	Seawater	0.146	0.041	0.018	12
Duplicate		0.144	0.071	0.044	7
Literature-1		0.144	0.057	0.043	5
Literature-1		0.139	0.048	0.039	6
Average		0.143	0.026	0.014	
Literature-2		0.100	0.305		22
Literature-4		0.020	0.140		6
Literature-4		0.050	0.170		5
Literature-4		0.120	0.130		5
Literature-5		0.030	0.170		55

Literature: 1 = Hu et al. (2018); 2 = Wang and Jacobsen (2016a); 3 = Wang and Jacobsen (2016b); 4 = Li et al. (2016); 5 = Morgan et al. (2018); 6 = Chen et al. (2019); 7 = Santiago Ramos et al. (2018). Replicate: repeat sample dissolution, column chemistry and instrumental analyses; duplicate: repeat analysis on the same purified sample solution during different analytical sessions. All data in this table are presented relative to NIST SRM 3141a. Data in literature 2 and 3 were measured against Merck Suprapur K, which has been confirmed by Literature 6 to have an identical $\delta^{41}K$ value to that of NIST SRM 3141a; therefore, no conversion is needed. Data in literature 1, 4, and 6 were measured against NIST SRM 3141a. Data in literature 5 and 7 were measured against NIST SRM 999b and were normalized relative to seawater. Since that NIST SRM 3141a is prepared from NIST SRM 999a, the K isotopic compositions of the two standards are assumed to be the same. Based on the K isotopic difference between seawater and NIST SRM 999b, we normalize $\delta^{41}K_{seawater}$ to $\delta^{41}K_{3141a}$ by adding 0.03. Analytical uncertainties in literature 2 and 3 are reported as 2SE and are converted to 2SD here while uncertainties in this study are reported both as 2SD and 95% c.i.

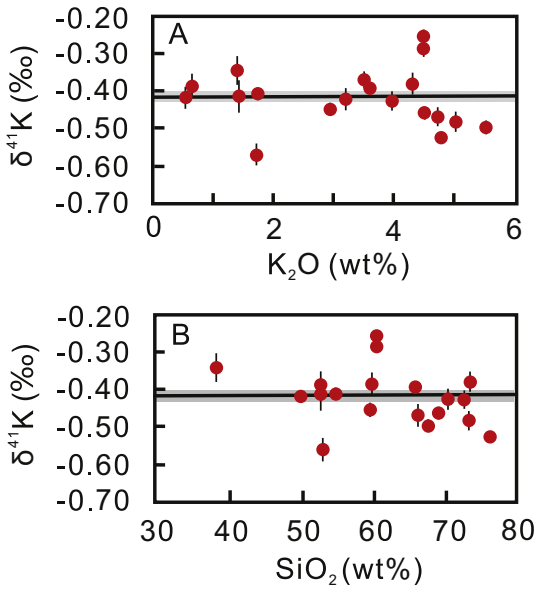

Fig. 5. K isotopic compositions of igneous reference materials vs K_2O (A) and SiO_2 (B). Error bar represents 95% c.i. The solid line and shaded area represent $\delta^{41}K$ of the mantle (−0.411 ± 0.012‰, 95% c.i.). $\delta^{41}K$ are reported in Table 3. K_2O and SiO_2 contents are from Govindaraju (1994).

narrow range from −0.416‰ for JB-1 to −0.348‰ for BR, which is consistent with previous analyses of basalts (Li et al., 2016; Wang and Jacobsen, 2016a; Morgan et al., 2018; Chen et al., 2019). Within all these igneous rock standards, there is no clear trend between $\delta^{41}K$ values and chemical indices of magma differentiation (e.g., K_2O and SiO_2 contents) (Fig. 5). This is opposite to the apparent positive correlation between $\delta^{41}K$ and SiO_2 values shown in Chen et al. (2019). Since the measured igneous rock standards are not genetically linked, our data suggest that in addition to magmatic differentiation, other factors such as source heterogeneity may also greatly affect the K isotopic composition of igneous rocks, particularly the more felsic ones.

Similar to most igneous rocks, the mica schist (SDC-1) has a $\delta^{41}K$ value of −0.461 ± 0.017‰, suggesting limited fractionation during metamorphic dehydration. The three shale standards show contrasting $\delta^{41}K$ values. The marine mud standard MAG-1 ($\delta^{41}K$ = −0.385 ± 0.025‰) and marine shale standard SCo-1 ($\delta^{41}K$ = −0.360 ± 0.025‰) fall at the high-$\delta^{41}K$ end of basalt range whereas the organic- and carbonate-rich shale SGR-1 is significantly heavier ($\delta^{41}K$ = −0.264 ± 0.015‰), reflecting the complex nature and origin of sedimentary rocks.

The Hawaiian seawater has an average $\delta^{41}K$ value of 0.143 ± 0.013‰, which is ~0.55‰ heavier than igneous rocks and suggests large isotope fractionations occur during fluid-rock interactions. Furthermore, out data agree with published results for several seawater samples from other oceans (Li et al., 2016; Wang and Jacobsen, 2016a; Morgan et al., 2018), indicating that K in seawater is well mixed and has a homogenous isotopic composition.

5. Conclusions

In this study, we report high-precision K isotopic data for seawater and 23 widely used and commercially available geological reference materials that include major lithological types. The K isotope compositions in 11 of the reference materials have not been previously analyzed and for 12 reference materials with published values, higher precision data are provided. The robustness of the cation exchange column chemistry (Bio-Rad AG50W-X8, 200–400 mesh resin) in 0.5 N HNO_3 was confirmed in three sets of tests using both synthetic solutions and natural rock standards. The $\delta^{41}K$ values range from −0.562‰ to −0.253‰ in 23 rock standards, while seawater has the highest $\delta^{41}K$ value of 0.143‰. Notably, the large K isotopic variation among the different lithologies that the standards represent suggests significant K isotope fractionation occurs during both low-temperature and high-temperature processes.

Acknowledgement

We thank Aaron Brewer, Zhe Yang, Ning Yang, William L. Fleming, Nicolas Cuozzo, Yang Sun, Chuan-Wei Zhu, Dong-Yong Li, Hao Yan, Mao-Yong He and Jing-Jing Yan for help in the laboratory and comments on the writing. Constructive and detailed comments from Leah Morgan, Weiqiang Li and an anonymous reviewer, and efficient editorial handling by Catherine Chauvel are gratefully acknowledged. This work was financially supported by the National Natural Science Foundation of China (Grants 41773064, 41503065, 41490635), XDPB11-01 and West Light Foundation of The Chinese Academy of Sciences.

References

Berglund, M., Wieser, M.E., 2011. Isotopic compositions of the elements 2009 (IUPAC technical report). Pure Appl. Chem. 83, 397–410.
Chen, H., Tian, Z., Brenna, T.-R., Randy, L.K., Wang, K., 2019. High-precision potassium isotopic analysis by MC-ICP-MS: an inter-laboratory comparison and refined K atomic weight. J. Anal. At. Spectrom. 34, 160–171.
Culkin, F., Cox, R., 1966. Sodium, potassium, magnesium, calcium and strontium in sea water. Deep-Sea Research and Oceanographic Abstracts 13, 789–804.
Edelmann, L., 1971. Method to examine adsorption of potassium, rubidium and cesium to cell membranes. Biophysik 7, 247–250.
Garner, E.L., Machlan, L.A., Barnes, I.L., 1975. The isotopic composition of lithium, potassium, and rubidium in some Apollo 11, 12, 14, 15 and 16 samples. Proc. Sixth Lunar Sci. Conf., pp. 1845–1855.
Govindaraju, K., 1994. Compilation of working values and sample description for 383 geostandards. Geostand. Newslett. 18, 1–158.
Hu, Y., Chen, X.-Y., Xu, Y.-K., Teng, F.-Z., 2018. High-precision analysis of potassium isotopes by HR-MC-ICPMS. Chem. Geol. 493, 100–108.
Humayun, M., Clayton, R.N., 1995a. Potassium isotope cosmochemistry: genetic implications of volatile element depletion. Geochim. Cosmochim. Acta 59, 2131–2148.
Humayun, M., Clayton, R.N., 1995b. Precise determination of the isotopic composition of potassium - application to terrestrial rocks and lunar soils. Geochim. Cosmochim. Acta 59, 2115–2130.
Li, W.Q., 2017. Vital effects of K isotope fractionation in organisms: observations and a hypothesis. Acta Geochimica 36, 374–378.
Li, W.Q., Beard, B.L., Li, S.L., 2016. Precise measurement of stable potassium isotope ratios using a single focusing collision cell multi-collector ICP-MS. J. Anal. At. Spectrom. 31, 1023–1029.
Li, W.Q., Kwon, K.D., Li, S.L., Beard, B.L., 2017. Potassium isotope fractionation between K-salts and saturated aqueous solutions at room temperature: laboratory experiments and theoretical calculations. Geochim. Cosmochim. Acta 214, 1–13.
McDonough, W.F., Sun, S.S., 1995. The composition of the Earth. Chem. Geol. 120, 223–253.
Morgan, L.E., Gordon, G.W., Arrua, R.C., Skulan, J.L., Anbar, A.D., Bullen, T.D., 2011. High-precision measurement of variations in calcium isotope ratios in urine by Multiple Collector Inductively Coupled Plasma Mass Spectrometry. Anal. Chem. 83, 6956–6962.
Morgan, L.E., Ramos, D.P.S., Davidheiser-Kroll, B., Faithfull, J., Lloyd, N.S., Ellam, R.M., Higgins, J.A., 2018. High-precision $^{41}K/^{39}K$ measurements by MC-ICP-MS indicate terrestrial variability of $\delta^{41}K$. J. Anal. At. Spectrom. 33, 175–186.
Parendo, C. A., Jacobsen, S.B., Wang, K., 2017. K isotopes as a tracer of seafloor hydrothermal alteration. Proceedings of the National Academy of Sciences, 114: 1827–1831.
Platzner, I.T., 1997. Modern Isotope Ratio Mass Spectrometry. (Chichester).
Richter, F.M., Watson, E.B., Chaussidon, M., Mendybaev, R., Christensen, J.N., Qiu, L., 2014. Isotope fractionation of Li and K in silicate liquids by Soret diffusion. Geochim. Cosmochim. Acta 138, 136–145.
Rudnick, R., Gao, S., 2003. Composition of the continental crust. Treatise on Geochemistry 3, 1–64.
Russell, W.A., Papanastassiou, D.A., 1978. Calcium isotope fractionation in ion-exchange chromatography. Anal. Chem. 50, 1151–1154.
Santiago Ramos, D.P., Morgan, L.E., Lloyd, N.S., Higgins, J.A., 2018. Reverse weathering in marine sediments and the geochemical cycle of potassium in seawater: insights from the K isotopic composition ($^{41}K/^{39}K$) of deep-sea pore-fluids. Geochim. Cosmochim. Acta 236, 99–120.
Strelow, F.W.E., Toerien, F.V.S., Weinert, C.H.S., 1970. Accurate determination of traces of sodium and potassium in rocks by ion exchange followed by atomic absorption spectroscopy. Anal. Chim. Acta 50, 399–405.
Taylor, T.I., Urey, H.C., 1938. Fractionation of the lithium and potassium isotopes by chemical exchange with zeolites. J. Chem. Phys. 6, 429–438.

Teng, F.-Z., Wadhwa, M., Helz, R.T., 2007. Investigation of magnesium isotope fractionation during basalt differentiation: implications for a chondritic composition of the terrestrial mantle. Earth Planet. Sci. Lett. 261, 84–92.
Teng, F.-Z., Dauphas, N., Watkins, J.M., 2017. Non-traditional stable isotopes: retrospective and prospective. Rev. Mineral. Geochem. 82, 1–26.
Wang, K., Jacobsen, S.B., 2016a. An estimate of the bulk silicate earth potassium isotopic composition based on MC-ICPMS measurements of basalts. Geochim. Cosmochim. Acta 178, 223–232.
Wang, K., Jacobsen, S.B., 2016b. Potassium isotopic evidence for a high-energy giant impact origin of the Moon. Nature 538, 487–490.
Zhang, Z.Y., Ma, J.L., Zhang, L., Liu, Y., Wei, G.J., 2018. Rubidium purification via a single chemical column and its isotope measurement on geological standard materials by MC-ICP-MS. J. Anal. At. Spectrom. 33, 322–328.